Hybrid Guided-Wave/Free-Space Optics Photonic Spectral Processor Based on LCoS Phase Only Modulator

David Sinefeld and Dan M. Marom, *Senior Member, IEEE*

***Abstract*—We propose and demonstrate a photonic spectral processor for applying arbitrary spectral phase and amplitude at high resolution with a 100-GHz free-spectral range for colorless wavelength-division-multiplexing adaptive filtering applications. The system employs free-space optics for projecting the dispersed light coming out of a planar-lightwave circuit onto a phase spatial-light modulator. The processor achieves 3-GHz optical resolution over 75-GHz usable bandwidth, with 557-MHz addressable granularity.**

***Index Terms*—Optical communication, optical filters, optical planar waveguide components, optical waveguide components.**

I. Introduction

OPTICAL devices for impairment mitigation are important for maximizing the performance of optical communication systems. With increasing channel transmission rates, the broad signal spectrum is susceptible to filtering and dispersion, resulting in a degraded signal reaching the receiver. Many device classes address impairment sources by offering tunable dispersion compensation (TDC) [1], [2] or optical equalization [3], in either guided-wave or free-space optical solutions. The concept of combing a dispersive element together with spatial light modulators (SLMs) were used for pulse shaping [4], power equalization [5], [6], add–drop switch [7], amplitude and time control [8], and spectral filtering [9], [10].

Dispersion compensation can be achieved by applying a quadratic phase function across a spatially dispersed optical spectrum. When a planar lightwave circuit (PLC) device employing a waveguide grating router (WGR) for dispersing the optical signal is used, the quadratic phase has to be applied at the output curved surface of the second slab lens. Several devices based on this concept have been demonstrated, using a polymer thermo-optic lens [11], or a deformable mirror [12] as the phase modulator. Recently [13], we presented a WGR-based device using a liquid crystal on silicon (LCoS), two-dimensional phase array modulator. With the LCoS SLM, we are able to prescribe arbitrary phase as well as amplitude to the signal's spectral components. We use external free-space optics to flatten and magnify the spectrum from the curved surface to a flat field incident on the LCoS array. The beam curvature introduced by the free-space optics section compensates for the WGR's curved output plane and magnifies the signal which allows us to achieve addressable spectral granularity of 557 MHz/pixel column.

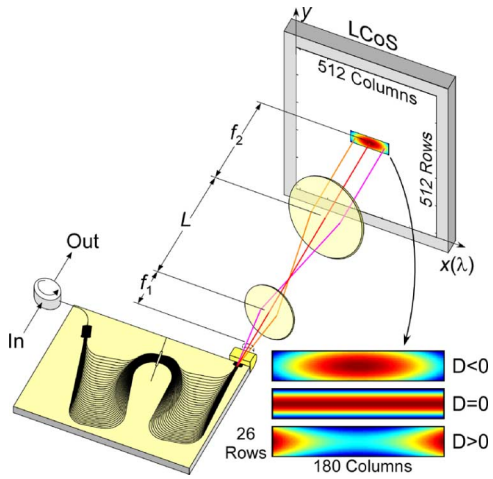

Fig. 1. Layout of the PSP. Spectrally dispersed light at the dashed curved surface are projected onto the LCoS SLM at a normal incidence angle. Inset: LCoS phase patterns sent to SLM. Horizontal curvature maps to dispersion; fixed vertical curvature is required for reduced losses. The illuminated area is small in comparison to the SLM.

In this letter, we provide further design details and updated measurement results of our photonic spectral processor (PSP). The updated results show a 17-dB loss improvement from our previous results [13], by introducing a vertical phase curvature using the SLM, to counter the beam curvature in the nondispersion direction. We now show that the optical resolution of our system is fundamentally limited by the resolving power of the WGR, providing 3-GHz resolution over a 75-GHz usable bandwidth with a 100-GHz free-spectral range (FSR). The functionality and performance of the PSP make it well suited for mitigating signal impairments and also for high resolution spectral carving or flattening.

II. System Design

The PSP layout is shown in Fig. 1. Light enters a PLC containing a high-resolution WGR through the "I/O" waveguide. Normally the light would be dispersed at the output curved surface of the second slab lens. However, since the PLC is cut through the slab lens, the refracted light focuses in air along a virtual curved surface residing off-chip (see dashed curved line

Manuscript received September 08, 2009; revised December 08, 2009; accepted January 17, 2010. First published February 02, 2010; current version published March 10, 2010. This work was supported in part by the Israel Science Foundation (Grant 1359/07) and in part by The Peter Brojde Center for Innovative Engineering.

The authors are with the Applied Physics Department, The Hebrew University of Jerusalem, Jerusalem 91904, Israel (e-mail: sinefeld@gmail.com; danmarom@cc.huji.ac.il).

Color versions of one or more of the figures in this letter are available online at http://ieeexplore.ieee.org.

Digital Object Identifier 10.1109/LPT.2010.2041548

in Fig. 1). The employed high-resolution WGR has been reused from [12], consisting of 34 grating arms. The on-chip slab lens radius is 3 mm, which reduces to ∼2 mm after refraction at the glass–air interface.

Normally, a reflective modulator would be placed along the curved surface with an ideal curvature matching that of the WGR curvature. Mirror deviations from the WGR curvature will result in spectral phase modulation, and can be designed for chromatic dispersion (CD) compensation [12]. In our system, we replaced the curved mirror with a phase-only, two-dimensional LCoS reflective modulator in order to achieve arbitrary spectral phase modulation and fine spectral granularity. However, placing the reflective SLM directly at the curved surface would imply that the SLM should be encoded with the WGR curvature for a flat frequency response. This would result in poor diffractive efficiency due to the multiple modulo 2π phase modulation wrapping.

Therefore, we project the spectrally dispersed curved surface onto a flat plane by using a free-space beam expander using lenses f_1 and f_2, separated by a distance L. The beam expander imparts a magnification of $M = f_2/f_1$ and phase curvature of $1/R = (f_1 + f_2 - L)/f_2^2$. A typical beam expander is set at $L = f_1 + f_2$, to prevent residual curvature. However, in our case, we wish to compensate for the curved input spectral surface (dashed line in Fig. 1), which is achieved by increasing the distance L, as shown in Fig. 1, resulting in the spectral components being dispersed along the SLM plane instead of the original curved surface. We use lenses of focal lengths $f_1 = 20$ mm and $f_2 = 200$ mm separated by $L = 420$ mm, which maps the input 2-mm field curvature onto a flat surface. Our choice of lenses magnifies both the spatial dispersion and the spot sizes by a factor of $M = 10$. The magnified spectral plane extends over 2.7 mm along the horizontal axis of the SLM. It is important to note that the beam emerging from the WGR is vertically collimated by a cylindrical lens. Since the beam expander is not in collimating condition, the outcoming beam carries a residual curvature of $R = 200$ mm in the y-axis, resulting in a high power loss. A phase curvature must be added along the vertical axis of the SLM in order to achieve high system transmissivity, which was absent in our early trial [13] and yields in a 17-dB loss improvement.

Our LCoS modulator (Boulder Nonlinear Systems Model P512–1550, based on nematic liquid crystal) is optimized for 1550-nm operation and has square pixels of 15-μm pitch, resulting in ∼180 columns spanning the 100-GHz-wide spectrum. Each column of the modulator addresses a particular center frequency, at 557-MHz shift in center frequency, given the system spatial dispersion of $dx/d\lambda = 3.35$ [mm/nm]. On the vertical axis, the beam is projected on 26 rows (or 390 μm). Phase modulation is achieved by prescribing an identical phase offset to all pixels in the column (on top of the curvature). Amplitude modulation can be achieved by several ways: modification of the curvature value, introduction of a linear phase ramp, or the application of a discrete phase jump, all performed in the vertical direction. System modulation speed is limited by our LCoS modulator model to 10 Hz.

The LCoS modulator supports one polarization only. Our free-space section provides ample space for a polarization diversity solution to be placed between the two lenses. However, one was not employed in the present PSP.

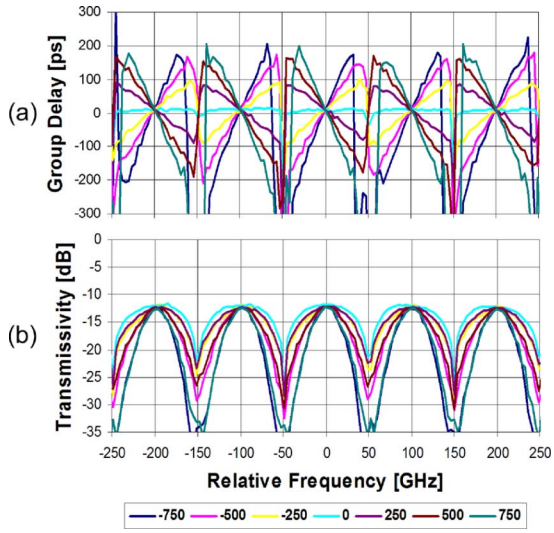

Fig. 2. Quadratic phase (CD compensation) results. (a) Group delay versus frequency. Linear slopes are observed, corresponding to seven different dispersion values (±750, ±500, ±250, and 0 ps/nm). (b) Transmissivity versus frequency. Spectral narrowing is observed for larger departures from zero dispersion. Passband and dispersion settings are repeated at 100-GHz FSR.

III. Results

The elements of the PSP, consisting of the WGR PLC, the two lenses, and the LCoS modulator were assembled on an optical table. A circulator was used to separate the input and output light to the PLC. The lens separation L was optimized to maximize and flatten the bandwidth, and the distance was very close to the designed separation. The usable bandwidth of the PSP was found to be ∼75 GHz (see Fig. 2). The insertion loss of the PSP is about 12 dB comprised of 8-dB losses caused by the double-pass in the WGR [11], 2 dB due to the circulator and other fiber connectors, and 2 dB from free-space losses, losses from the SLM and high diffraction orders elimination.

To test the processor as a TDC, quadratic phase functions with varying radii were applied in the dispersion direction. The quadratic phase maps to CD values according to the equation: $\mathrm{CD} = 2\lambda_0/c_0(dx/d\lambda)^2 \cdot CV$, where $CV = 1/R$ is the phase curvature, and $dx/d\lambda$ is the spatial dispersion, achieving $\mathrm{CD} = 115\,600 \cdot CV$ [ps/nm] for our PSP implementation (where CV is measured in mm^{-1}). In order to measure the actual CD values that were applied by the PSP, we used a modulation phase shift (MPS) setup with a tunable laser. The group delay results for several CD values are shown [Fig. 2(a)]. Higher CD values result in spectral narrowing [Fig. 2(b)]. The CD values and −3-dB pass bandwidth as a function of the phase curvature are shown in Fig. 3. It can be seen that CD values are linearly dependent on phase curvature, and that narrowing effect becomes more pronounced. Bandwidth is reduced down to 30 GHz for CD values of ±750 ps/nm. Note that the passband can be artificially widened by imparting additional loss [Fig. 5(a)].

To characterize the spectral resolution of the PSP, an abrupt π phase jump was applied to one part of the signal spectrum. Spectral components near the abrupt phase transition experience a coupling loss, from which both the spatial dispersion and the resolution can be extracted (Fig. 4). The −3-dB bandwidth of the minimum resolvable spectral feature, or the optical resolution, was found to be 3 GHz. This result correlates well with the

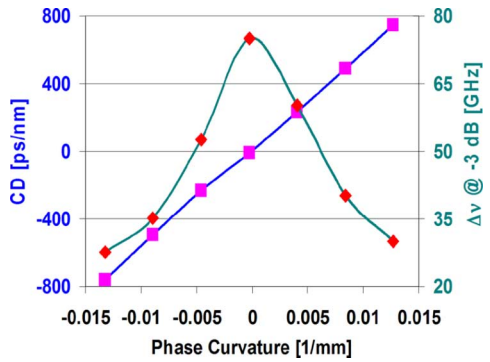

Fig. 3. CD values (blue) and bandwidth (green) versus curvature. As the phase curvature values are larger, the narrowing effect becomes dominant and the bandwidth is reduced down to 30 GHz for CD values of ±750 ps/nm.

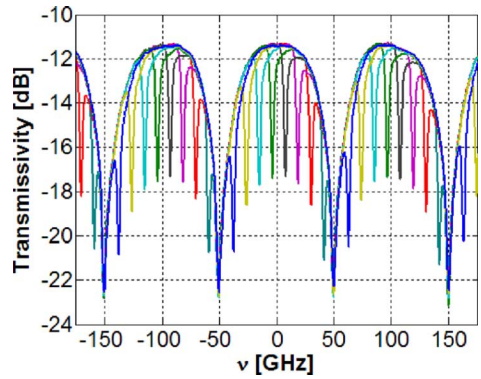

Fig. 4. Optical spectrum of PSP when testing for optical resolution. A narrow spectral dip is scanned across the spectrum. Dip width of 4.1 GHz is an artifact of the finite OSA resolution. Actual dip, measured with scanning laser, is 3 GHz wide.

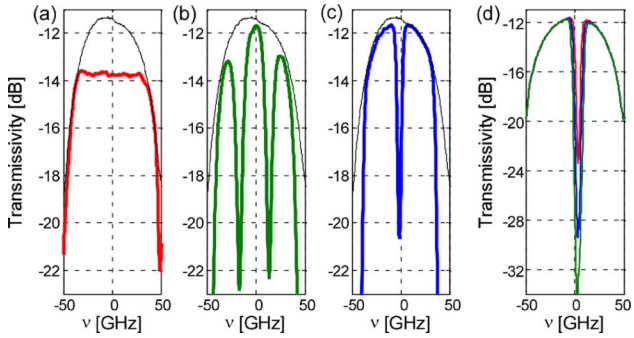

Fig. 5. Demonstration of spectral carving across the channel bandwidth, where black line denotes the native spectrum. (a) Spectral flattening; (b) spectrum carved to three sub-bands; (c) spectrum narrowed at edges and a narrow notch inserted; and (d) narrow attenuation exhibiting 22-dB dynamic range.

WGR resolvability, equaling the FSR divided by the WGR arm count (100/34, respectively).

Since the introduction of the LCoS array allows us to prescribe both spectral phase and amplitude modulation, we demonstrate this functionality by imparting attenuation features onto the channel spectrum (Fig. 5). The technique can be used to attenuate spectral features and enhance the signal quality in the time domain [10] or optimally filter a signal which has undergone distortion due to multiple spectrally misaligned channelized components. Any spectral shape, subject to the constraint of the optical resolution, can be prescribed. The dynamic range of the attenuation is greater than 20 dB [Fig. 5(d)], limited mostly by back reflections from the PLC end. However, this result is resolution dependent. When operating a high-resolution pattern, the dynamic range is lower (Fig. 4) due to the SLM spatial response.

IV. Summary

We demonstrated the functionality of the PSP, which is capable of modulating a communication signal's spectral components in amplitude and phase. The spectral resolution of the PSP is determined by the WGR, which for the present realization resolves 3-GHz features with a 75-GHz usable bandwidth and a 100-GHz FSR. The resolution can be improved with the use of a WGR with a greater number of grating arms (i.e., larger PLC). The small pixel size of the modulator allows us to address fine spectral granularity, finer than the optical resolution. Hence, we can truly extract the performance potential of the WGR with this approach.

References

[1] M. Shirasaki, "Chromatic dispersion compensator using virtually im-aged phased array," *IEEE Photon. Technol. Lett.*, vol. 9, no. 12, pp. 1598–1600, Dec. 1997.

[2] K.-M. Feng, J.-X. Cai, V. Grubsky, D. S. Starodubov, M. I. Hayee, S. Lee, X. Jiang, A. E. Willner, and J. Feinberg, "Dynamic dispersion compensation in a 10-Gb/s optical system using a novel voltage tuned nonlinearly chirped fiber Bragg grating," *IEEE Photon. Technol. Lett.*, vol. 11, no. 3, pp. 373–375, Mar. 1999.

[3] C. R. Doerr, S. Chandrasekhar, P. J. Winzer, A. R. Chraplyvy, A. H. Gnauck, L. W. Stulz, R. Pafchek, and E. Burrows, "Simple multichannel optical equalizer mitigating intersymbol interference for 40-Gb/s non return-to-zero signals," *J. Lightw. Technol.*, vol. 22, no. 1, pp. 249–256, Jan. 2004.

[4] A. Krishnan, M. Knapczyk, L. Grave de Peralta, A. A. Bernussi, and H. Temkin, "Reconfigurable direct space-to-time pulse-shaper based on arrayed waveguide grating multiplexers and digital micromirrors," *IEEE Photon. Technol. Lett.*, vol. 17, no. 9, pp. 1959–1961, Sep. 2005.

[5] J. E. Ford and J. A. Walker, "Dynamic spectral power equalization using micro-opto-mechanics," *IEEE Photon. Technol. Lett.*, vol. 10, no. 10, pp. 1440–1442, Oct. 1998.

[6] N. Riza and M. J. Mughal, "Broadband optical equalizer using fault tolerant digital micromirrors," *Opt. Express Internet J.*, vol. 11, pp. 1559–1565, Jun. 2003.

[7] J. S. Patel and Y. Silberberg, "Liquid crystal and grating-based multiple wavelength cross- connect switch," *IEEE Photon. Technol. Lett.*, vol. 7, no. 5, pp. 514–516, May 1995.

[8] N. A. Riza and N. Madamopoulos, "Synchronous amplitude and time control for an optimum dynamic range variable photonic delay line," *Appl. Opt.*, vol. 38, pp. 2309–2318, Apr. 1999.

[9] M. C. Parker, A. D. Cohen, and R. J. Mears, "Dynamic digital holographic wave- length filtering," *J. Lightw. Technol.*, vol. 16, no. 7, pp. 1259–1270, Jul. 1998.

[10] N. A. Riza and S. A. Reza, "High-dynamic-range hybrid analog-digital control broadband optical spectral processor using micromirror and acousto-optic devices," *Opt. Lett.*, vol. 33, pp. 1222–1224, Jun. 2008.

[11] C. R. Doerr, R. Blum, L. L. Buhl, M. A. Cappuzzo, E. Y. Chen, A. Wong-Foy, L. T. Gomez, and H. Bulthuis, "Colorless tunable optical dispersion compensator based on a silica arrayed-waveguide grating and a polymer thermooptic lens," *IEEE Photon. Technol. Lett.*, vol. 18, no. 11, pp. 1222–1224, Jun. 1, 2006.

[12] D. M. Marom, C. R. Doerr, M. A. Cappuzzo, E. Y. Chen, A. Wong-Foy, L. T. Gomez, and S. Chandrasekhar, "Compact colorless tunable dispersion compensator with 1000-ps/nm tuning range for 40-Gb/s data rates," *J. Lightw. Technol.*, vol. 24, no. 1, pp. 237–241, Jan. 2006.

[13] D. Sinefeld and D. M. Marom, "Colorless photonic spectral processor using hybrid guided-wave/free-space optics arrangement and LCoS modulator," in *Proc. OFC*, San Diego, CA, 2009, Paper OThB4.